

HF radar technology in the Sea of Okhotsk

Naoto Ebuchi, Yasushi Fukamachi, Kay-Ichiro Ohshima and Masaaki Wakatsuchi

Institute of Low Temperature Science, Hokkaido University, Sapporo, Japan
E-mail: ebuchi@lowtem.hokudai.ac.jp

Abstract

In order to monitor variations in the Soya Warm Current (SWC), three high frequency (HF) radar stations were installed around the Soya Strait in August 2003. The radar covers a range of approximately 70 km from the coast. Comparisons of the observed current velocity with drifting buoy and shipboard ADCP data showed good agreement with root-mean-square differences of 20 cm/s. It is shown that the HF radars clearly capture seasonal variations of the SWC. The velocity of the SWC reaches its maximum, approximately 1 m/s, in summer, and weakens in winter. The velocity core is located 20 to 30 km from the coast, and its width is approximately 50 km. The almost same seasonal cycle was repeated in each of these five years from 2003 to 2008. Surface transport by the SWC shows a significant correlation with the sea level difference along the strait, as derived from coastal tide gauge records. The cross-current sea level difference, which is estimated from the sea level anomalies observed by the Jason-1 altimeter and a coastal tide gauge, also exhibits variation in concert with the surface transport and along-current sea level difference. In addition to the annual variation, the SWC exhibits subinertial variations with a period of 5–20 days.

Introduction

The Sea of Okhotsk (Fig. 1), a marginal sea adjacent to the North Pacific, is one of the southernmost seasonal sea ice zones in the Northern Hemisphere and it has been conjectured that it is a region in which the North Pacific Intermediate Water is ventilated to the atmosphere. The Sea of Okhotsk is connected with the Sea of Japan through the Soya/La Perouse Strait, which is located between Hokkaido, Japan, and Sakhalin, Russia. The Soya Warm Current (SWC) enters the Sea of Okhotsk from the Sea of Japan through the Soya Strait and flows along the coast of Hokkaido as a coastal boundary current. It supplies warm, saline water in the Sea of Japan to the Sea of Okhotsk. The current is roughly barotropic and shows a clear seasonal variation (Aota, 1984; Matsuyama *et al.*, 1999). However, the SWC has never been continuously monitored due to the difficulties involved in field observations related to various reasons, such as severe weather conditions in winter, political issues at the border strait, and conflicts with fishing activities in the strait. Detailed features of the SWC and its variations have not been clarified. Information concerning the variations of the SWC and the water exchange between the Sea of Japan and the Sea of Okhotsk is important for the study of both of these seas.

In this report, observation of the SWC using the HF radars is briefly introduced together with variations of the SWC revealed by a combination of the observed surface current fields with the sea level observations from coastal tide gauges and satellite altimetry. A detailed description of the HF radar system and validation of the observed surface current

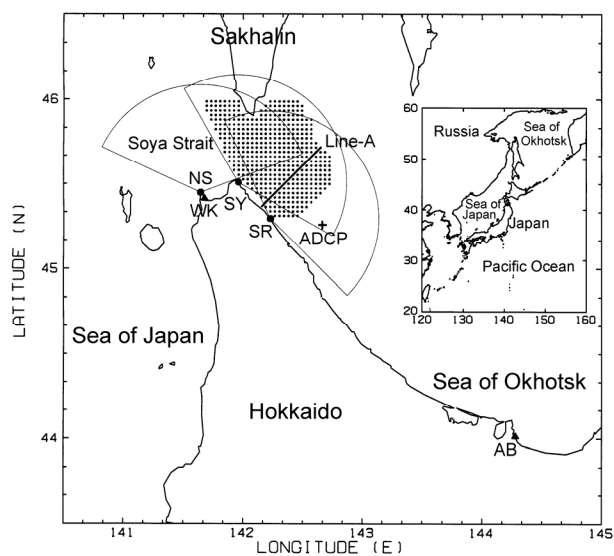


Fig. 1 Map of the Soya/La Perouse Strait, and location and coverage of the HF radar stations.

data were reported by Ebuchi *et al.* (2006). Fukamachi *et al.* (2008) estimated volume transport of the SWC using the surface current fields together with current velocity profiles observed by a bottom-mounted acoustic Doppler current profiler (ADCP). Ebuchi *et al.* (2008) investigated seasonal and subinertial variations in the SWC using data from HF radar, coastal tide gauges and bottom-mounted ADCP.

Observation of the SWC using the HF radar system

In order to continuously monitor the SWC, three HF radars (CODAR Ocean Sensors, SeaSonde) (Barrick *et al.*, 1977) were installed around the Soya Strait (Fig. 1). The frequency of the HF radar is 13.9 MHz, and the range and azimuth resolutions are 3 km and 5°, respectively. The HF radar covers a range of approximately 70 km from the coast. The observations were made at one-hourly intervals. We measured the beam pattern of the receiving antenna and corrected for distortion of the antenna pattern to derive accurate radial velocities. Surface current vectors were composed in grid cells of 3 × 3 km using the radial velocity components observed by the radars according to a least squares method.

An example of the observed surface current vector field is shown in Figure 2. Figure 3 is an example of the monthly-averaged surface current field. In these figures, the SWC, which flows from west to east across the Soya Strait and turns toward the southeast along the coast, is captured very clearly. They also show southward currents along the west coast of Sakhalin, as predicted by numerical experiments (Ohshima and Wakatsuchi, 1990; Ohshima, 1994).

The surface current velocity observed hourly by the HF radars was compared with *in-situ* data from drifting buoys and shipboard ADCPs (Ebuchi *et al.*, 2006). The current velocity derived from the HF radars showed good agreement with that observed using drifting buoys (Fig. 4). The root-mean-square differences were found to be less than 25 cm/s for the zonal and meridional components. The observed current velocity was also found to exhibit reasonable agreement with the shipboard ADCP data (Fig. 5).

Structure and seasonal variation of the Soya Warm Current

Using the surface current vector fields observed by the HF radars, we discuss seasonal variations of the

SWC. In order to remove the tidal constituents, a 25-h running average was applied to the time series of the hourly surface current vectors in each grid cell, and then daily and monthly mean current fields were calculated. To remove the tidal variations, we examined a 25-h running average, harmonic analysis, and 48-h tide killer filter, and confirmed that the residual of the tidal components are negligibly small. An example of the monthly-averaged field is shown in Figure 3.

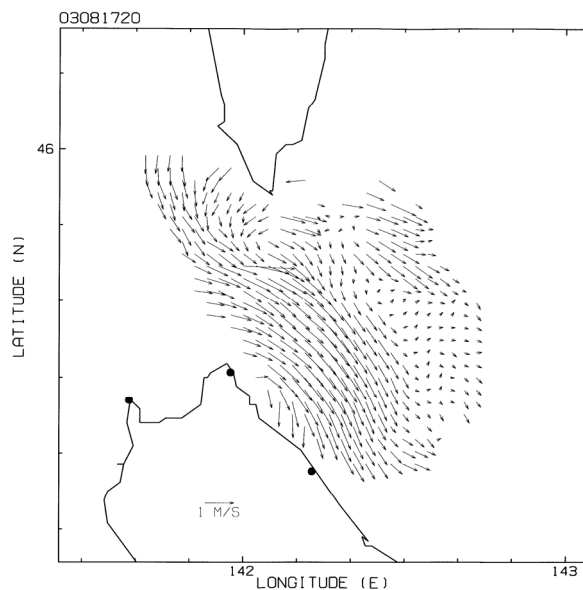


Fig. 2 An example of an hourly surface current vector field (1100 UTC, August 17, 2003).

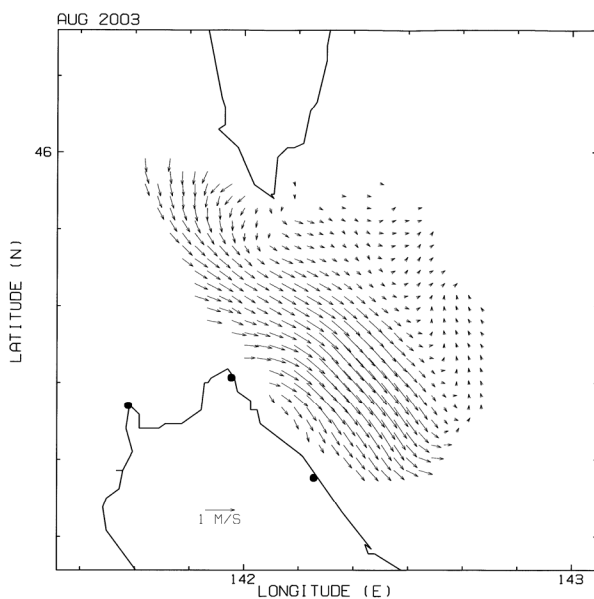


Fig. 3 An example of a monthly-averaged surface current field (August 2003).

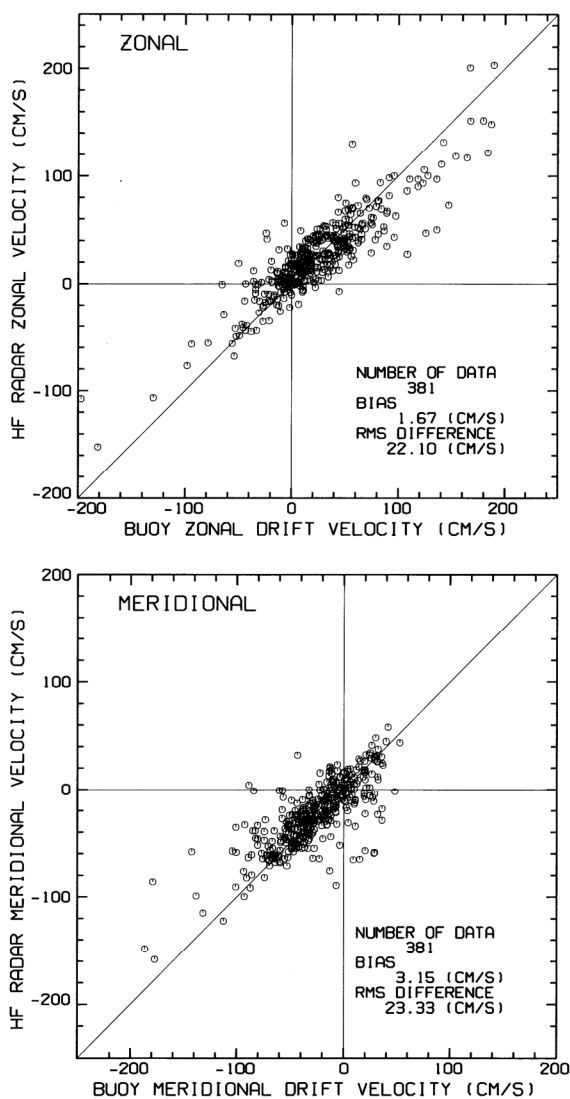


Fig. 4 Comparison of HF radar with drifting buoy observations for zonal (upper) and meridional (lower) velocity components.

Daily southeastward current components across Line-A (Fig. 1) were averaged monthly and are shown with standard deviations in Figure 6 for the period from August 2003 to July 2004. Figure 7 shows year-to-year variations of the monthly mean profiles within the five years from 2003 to 2008. The monthly-mean profiles show a clear seasonal variation. The velocity of the SWC reaches its maximum of approximately 1 m/s in summer (August and September) and becomes weak in winter (January and February). The current axis is located 20 to 30 km from the coast in this region, and the typical width of the SWC is approximately 50 km. These features of the SWC are consistent with the

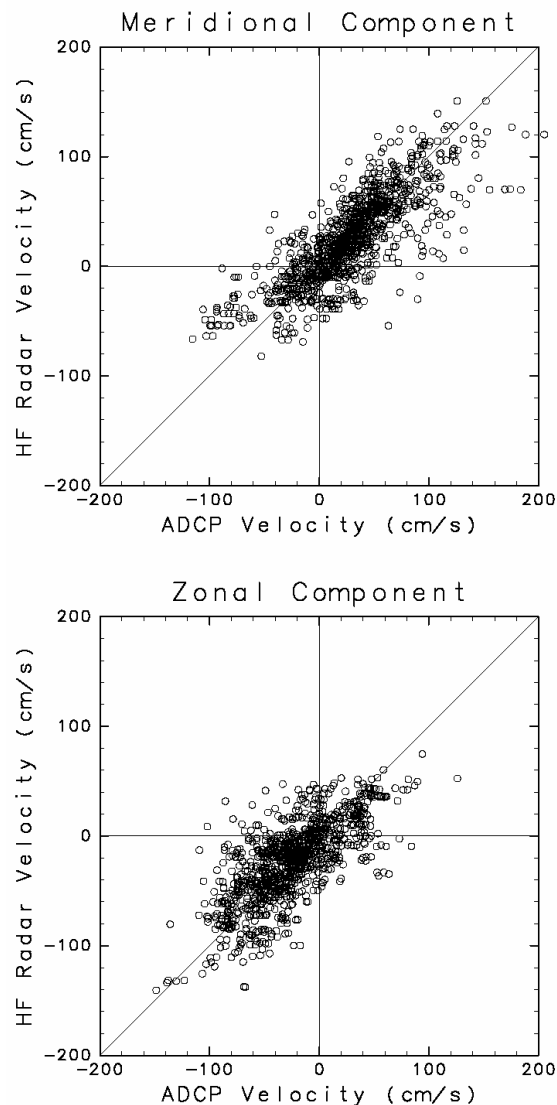


Fig. 5 Comparison of HF radar with shipboard ADCP observations for zonal (upper) and meridional (lower) velocity components.

results of short-term or point-wise observations reported in previous studies (Aota, 1984; Matsuyama *et al.*, 1999). In Figure 7 it is shown that the almost same seasonal cycle has been repeated in these five years.

Variations of the surface transport and their relationship with sea level differences

Daily surface transport across Line-A was defined by the integration of the daily southeastward current component along the line from the coast to a point at which the component becomes negative. Figure 8 shows the time series of the surface transport (thick

line). Note that the unit of surface transport is not volume/time but area/time because the HF radars provide only the surface current velocity. In winter (from January to March), there is often a lack of data because the observation region is covered by sea ice.

The driving force of the SWC is ascribed to the sea level difference between the Sea of Japan and the Sea of Okhotsk (Aota, 1984; Ohshima, 1994). The surface velocity of the SWC has been reported to be closely related to the sea level difference (Aota, 1984; Matsuyama *et al.*, 1999). For comparison with the surface transport, as observed by the HF radars, we calculated the sea level difference between two tide gauge stations, Wakkanai (labeled as WK in Fig. 1) and Abashiri (AB in Fig. 1), which represents the sea level difference between the Sea of Japan and the Sea of Okhotsk. A 48-hour tide-killer filter was applied to the hourly tide gauge records at these

stations. The daily-mean sea levels were then calculated, and atmospheric pressure correction was performed using the daily-mean sea level pressure observed at weather stations in the cities of Wakkanai and Abashiri. The time series is shown by a thin line in Figure 8. The surface transport of the SWC and the sea level difference along the current show a good correlation with a correlation coefficient of 0.702. Both time series exhibit not only the seasonal variation but also variations with time scales of approximately 10 to 15 days. The generation mechanism of this subinertial variation in the SWC was discussed by Ebuchi *et al.* (2008) in relation with wind-generated coastally trapped waves propagating along the east coast of Sakhalin and west coast of Hokkaido. The results shown in Figure 8 confirm the correlation at various time scales between the SWC and the along-current sea level difference.

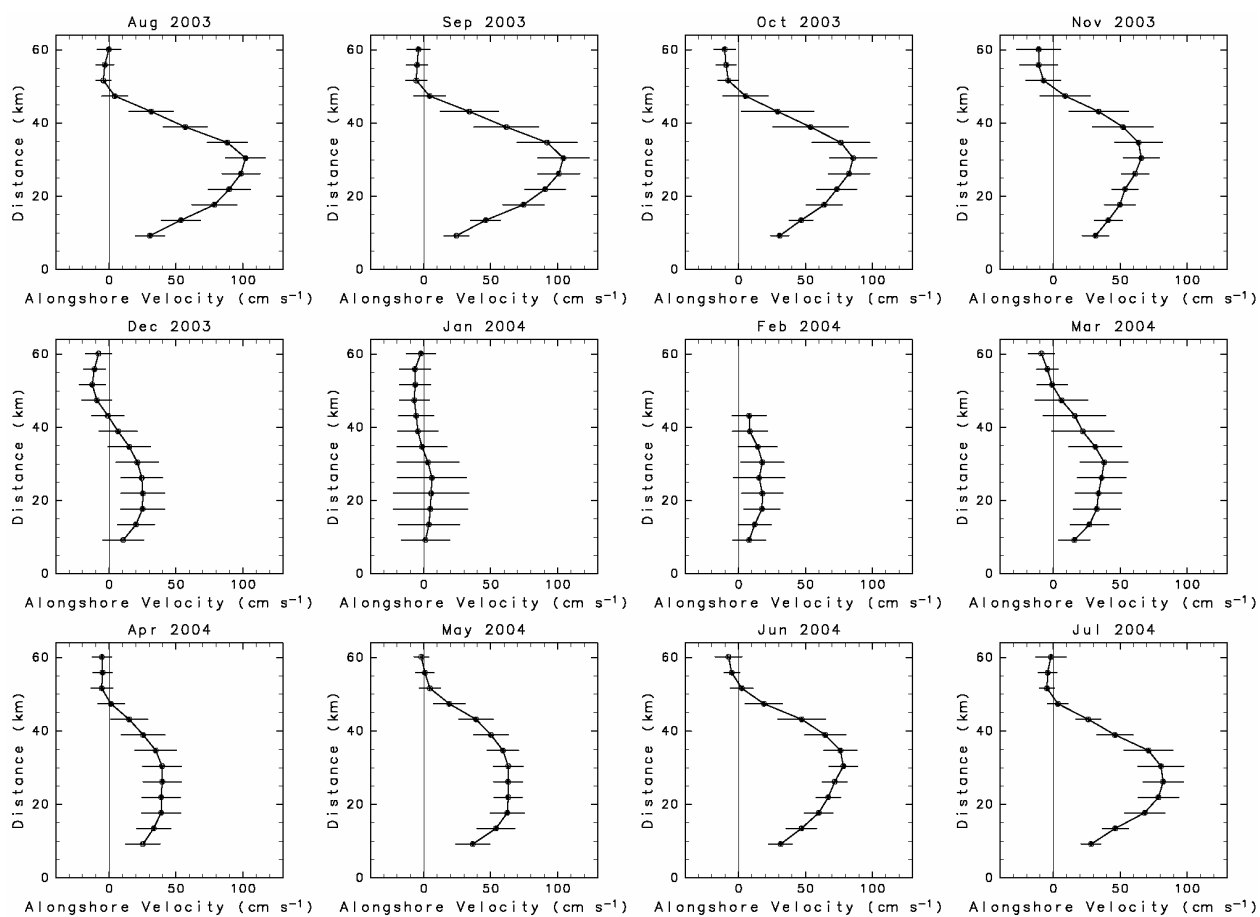


Fig. 6 Monthly-averaged profiles of the southeastward current velocity component across Line-A (Fig. 1) with respect to the distance from the coastline for the period from August 2003 to July 2004.

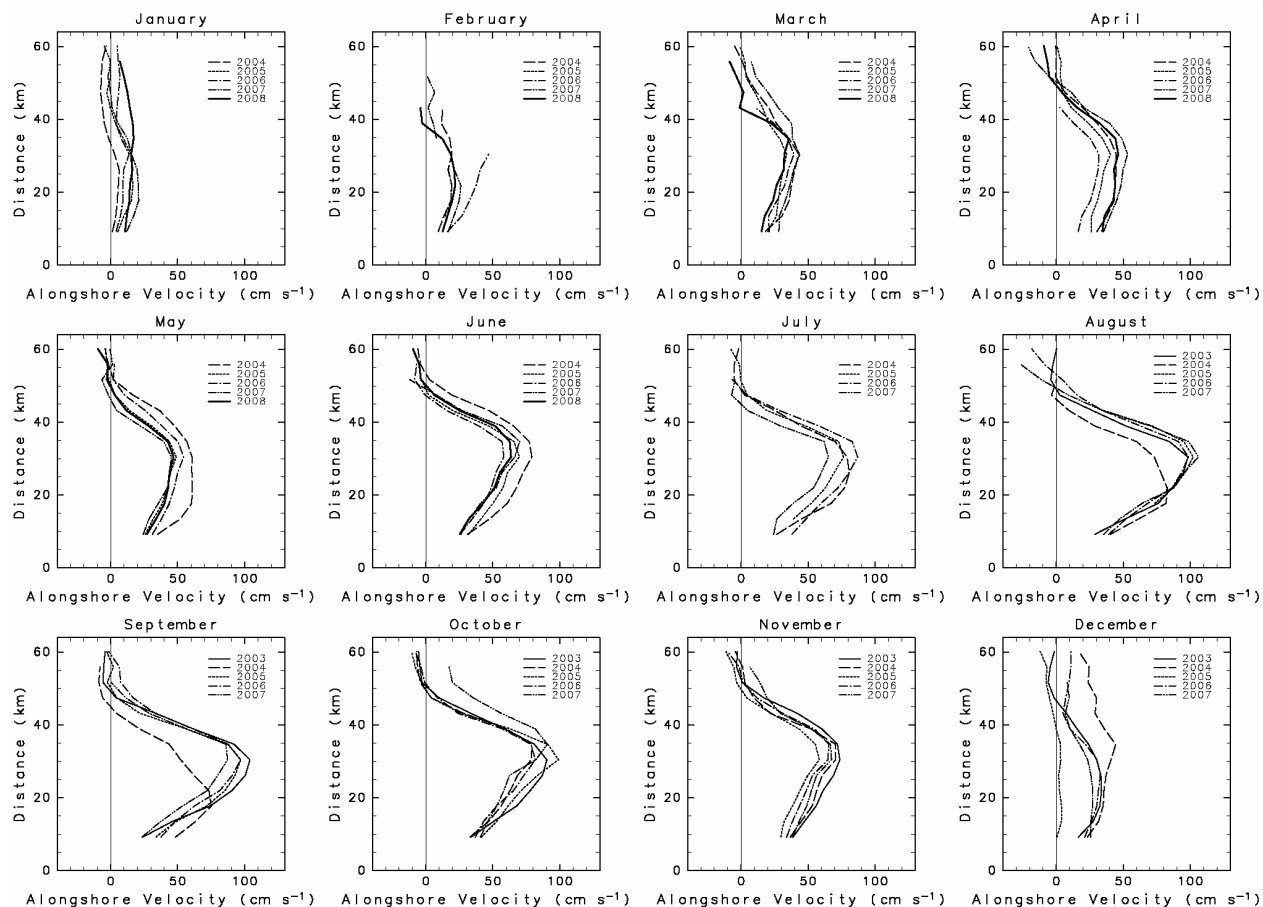


Fig. 7 Year-to-year variations of the monthly-averaged profiles of the southeastward current velocity component across Line-A (Fig. 1).

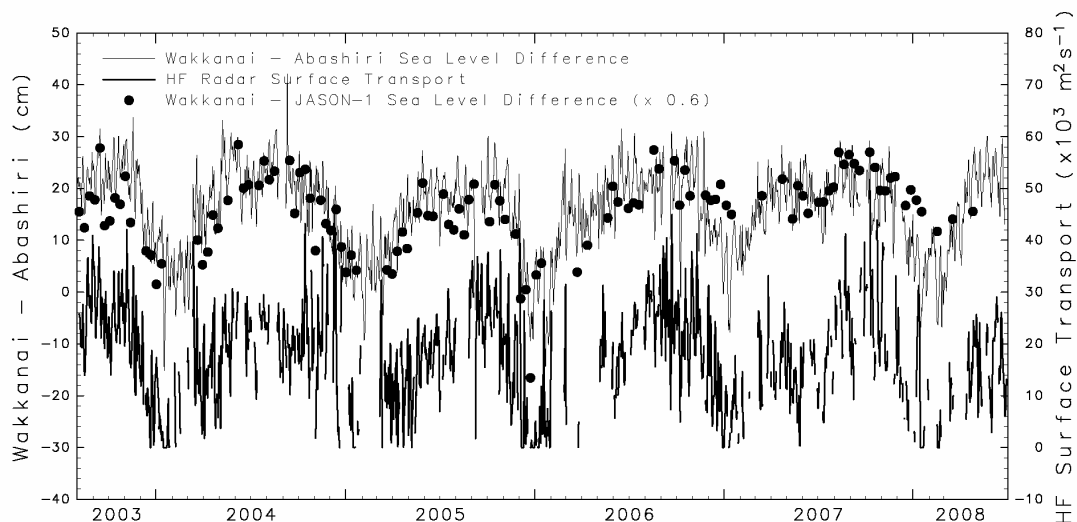


Fig. 8 Time series of the surface transport of the Soya Warm Current (SWC, thick line), the sea level difference between Wakkanai and Abashiri (thin line), and anomaly of the sea level difference between Wakkanai and the ground track B (Fig. 9) of the Jason-1 altimeter (solid circles).

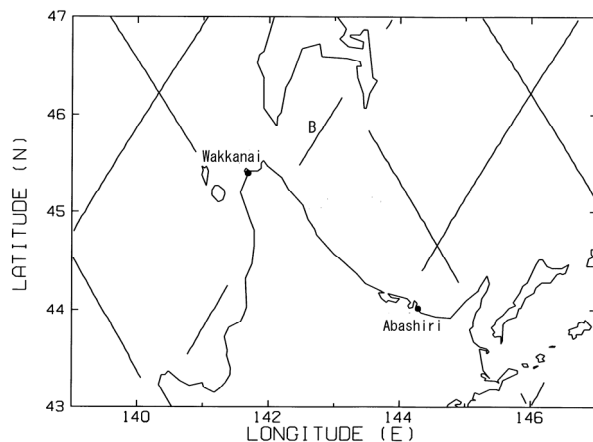


Fig. 9 Locations of ground tracks of the Jason-1 altimeter and tide gauge stations of Wakkainai and Abashiri.

In order to assess variations of the sea level difference in the cross-current direction, we utilized the sea level anomalies observed by the Jason-1 satellite altimeter. Figure 9 shows locations of ground tracks of Jason-1 in the Sea of Okhotsk. Since the spaceborne radar altimeter is not able to observe the sea surface height accurately in the region close to the coastline, we cannot obtain the cross-current sea surface height profiles associated with the SWC directly from the altimeter data. Therefore, the difference of the sea level anomalies between the offshore observations by the altimeter (indicated by B in Fig. 9) and the coastal tide gauge records at the Wakkainai station is utilized to represent the sea level variations across the SWC.

In Figure 8, the variation of sea level difference across the SWC is indicated by solid circles. The amplitude of the cross-current sea level difference is multiplied by 0.6 and is shifted vertically to match with the along-current sea level difference (thin line) in Figure 8. The temporal interval of the Jason-1 observation is 9.91 days. It is shown that the cross-current sea level difference is well correlated with the along-current sea level difference and also with the surface transport of the SWC. These results support evidence that the SWC is in geostrophic balance in the cross-current direction, and is driven by the sea level difference between the Sea of Japan and the Sea of Okhotsk (Aota, 1984). The same

relationship between the cross- and along-current sea level differences were discernible in the 10-year record of the sea level anomaly obtained by the TOPEX/Poseidon altimeter combined with the coastal tide gauge records (not shown here).

Concluding Remarks

In this report, we briefly introduced the HF radar system deployed in the Soya/La Perouse Strait region and analyses of the observed surface velocity fields. The HF radars clearly captured seasonal and subinertial variations in the SWC. It is demonstrated that HF radar system is a powerful tool to monitor surface current fields in coastal regions.

References

- Aota, M. 1984. Oceanographic structure of the Soya Warm Current. *Bull. Coast. Oceanogr.* **22**: 30–39 (in Japanese).
- Barrick, D.E., Evans, M.W. and Weber, B.L. 1977. Ocean surface currents mapped by radar. *Science* **198**: 138–144.
- Ebuchi, N., Fukamachi, Y., Ohshima, K.I., Shirasawa, K., Ishikawa, M., Takatsuka, T., Daibo, T. and Wakatsuchi, M. 2006. Observation of the Soya Warm Current using HF radar. *J. Oceanogr.* **62**: 47–61.
- Ebuchi, N., Fukamachi, Y., Ohshima, K.I. and Wakatsuchi, M. 2009. Subinertial and seasonal and variations in the Soya Warm Current revealed by HF ocean radars, coastal tide gauges and a bottom-mounted ADCP. *J. Oceanogr.* **65**: 31–43.
- Fukamachi, Y., Tanaka, I., Ohshima, K.I., Ebuchi, N., Mizuta, G., Yoshida, H., Takayanagi, S. and Wakatsuchi, M. 2008. Volume transport of the Soya Warm Current revealed by bottom-mounted ADCP and ocean-radar measurement. *J. Oceanogr.* **64**: 385–392.
- Matsuyama, M., Aota, M., Ogasawara, I. and Matsuyama, S. 1999. Seasonal variation of Soya Current. *Umi no Kenkyu* **8**: 333–338 (in Japanese with English abstract and captions).
- Ohshima, K.I. and Wakatsuchi, M. 1990. A numerical study of barotropic instability associated with the Soya Warm Current in the Sea of Okhotsk. *J. Phys. Oceanogr.* **20**: 570–584.
- Ohshima, K.I. 1994. The flow system in the Sea of Japan caused by a sea level difference through shallow straits. *J. Geophys. Res.* **99**: 9925–9940.